# Generic studies for industrial heat exchanger fouling

Development of a Pilot-monitor

Reference number 93-023
File number 112325-21869
Date January 1993
NP

Authors
H.C. van Deventer [1)]
S.I. Timmerman [1)]
J.R. van der Vliet [2)]

Contract JOUE - 0040 - C

Attended for
The Commission of the European Communities
Directorate-General for science research and development
Brussels
Belgium

Novem Utrecht
P.O.Box 8242
3503 RE Utrecht
Novem contract no. 33105/0010 and 33105/0011

---

1) TNO Institute of Environmental and Energy Technology
Department of Heat and Refrigeration Technology
P.O. Box 342
7300 AH Apeldoorn
The Netherlands

2) Institute of Environmental Sciences
Sensor group
P.O. Box 6011
2600 JA Delft
The Netherlands

## Summary

As part of the European CEC Project Joue-0040-C 'Generic Studies for Industrial Heat Exchanger Fouling' a study was undertaken to develop a gas-side fouling pilot monitor.

The monitor device is designed to provide an indication of the progress of fouling within a heat exchanger. The increase of the temperature and the change of the emission coefficient of the heat exchanger surfaces indicate fouling.
The measuring principle for the monitor is the measurement of infra-red radiation emitted from the fouled surface of a heat exchanger at three or more wavelengths. The temperature and the emissivity of the fouled surface are computed by iterative fitting of the Planck equations.
A camera set-up is selected. This presents the possibility of obtaining images of streaks of the surface, thus measuring the temperature and the emissivities at different locations on a fouled heat exchanger pipe.
A laboratory test facility is set up in order to test the principle of the monitor. The aim of the laboratory tests is to verify the surface temperatures and the emission coefficients measured and calculated by the monitor.
The results of the laboratory tests showed that the temperatures calculated by the software differ in some cases by more than 10 °C from the temperature measured by a thermocouple and that the emission coefficient in some cases differs by more than 10 % from the real emission coefficient. These large differences are probably caused by the relatively large fluctuations in the measured data. Expectations are that improvement in the stability of the measuring method will improve the quality of the input data of the iteration program. This will probably result in a more exact calculation of the surface temperatures and emission coefficients.

## Table of Contents

# 1 Objective

The objective of this study is to develop a measuring method suitable for monitoring the gas-side fouling of industrial heat exchangers.
A measuring method was chosen which is based on the measurement of infrared radiation emitted from a fouled surface. It is possible to determine the temperature and emissivity of a heat exchanger surface with the data of emitted radiation.
A laboratory test facility is set up. With the laboratory tests we aim to verify the surface temperatures and the emission coefficients measured and calculated by the monitor. The surface temperature is therefore also measured by a thermocouple. The emission coefficient is determined separately by two infrared cameras.

# 2 Introduction

In general fouling is the main cause of diminishing efficiency of a heat exchanger and can therefore also result in economic loss.
The project "Generic studies for industrial heat exchanger fouling", contract JOUE - 0040 - C, has as its main objective the development, construction and validation of mathematical models which may be used to predict the extent of gas-side heat exchanger fouling for a variety of environments. In addition a practical fouling monitor has been designed. This monitor in combination with the mathematical models enables the user to judge the fouling of the surface.

The monitor device is designed to give an indication of the progress of fouling within a heat exchanger. The increase in the temperature and the change of the emission coefficient of the heat exchanger surface indicate fouling. An optical, infrared principle is selected as the most suitable measuring principle because it can measure temperatures without contact.
The monitor measures the infrared radiation emitted by a heat exchanger surface and calculates the temperature and emissivity.
The project is divided into two parts. The first part of the investigation covers the development of the method and the design of the camera. The selection of the measuring principle and the theoretical background of the principle are described in chapter 5.1 and 5.2. The practical design of the monitor, covering the selection of the infrared detector and the choice of the filters, is described in 5.3. The software needed to calculate the temperatures and the emission coefficients from the measured radiation is also described in chapter 5.3.
The second part of the investigation covers the testing and verification of the monitor. For this purpose a laboratory test facility is set up. The experimental test set-ups and the measuring equipment are described in chapter 5.4.
Experiments have been done on one test tube. Results of these experiments are described in chapter 6.

# 3 Conclusions

A method for the monitoring of gas-side fouling based on infrared emission of heat exchanger surfaces has been developed. A monitor based on this method for the measurement of surface temperatures and emissivities has been designed and built. The temperature and emissivity are calculated from Planck's equation through iteration with the aid of a computer.

The monitor is still too vulnerable to be used under industrial conditions. The monitor has to be shielded from dust, water and aggressive components.

The results of the tests with the monitor showed that the response of the monitor is not constant in time and that the measuring data exhibit rather large fluctuations.

The results of the laboratory tests showed that the temperatures calculated by the software differ in some cases by more than 10 °C from the temperature measured by a thermocouple and that the emission coefficient in some cases differs by more than 10 % from the real emission coefficient. These large differences are probably caused by the relatively large fluctuations in the measured data.

# 4 Table of symbols

| | | |
|---|---|---|
| B | = the measured radiation energy | [W/m$^2$] |
| h | = Planck's constant | [Js] |
| c | = speed of light | [m/s] |
| k | = Boltzmann's constant | [J/K] |
| n | = number of experiments | [-] |
| r | = transmission | [-] |
| $T_o$ | = surface temperature | [K] |
| $T_e$ | = environment temperature | [K] |
| Q | = intensity of radiation | [W/m$^2$] |
| | | |
| $\varepsilon$ | = emission coefficient | [-] |
| $\lambda$ | = wavelength | [m] |
| $\sigma$ | = Stefan-Boltzmann's constant | [W/m$^2$K$^4$] |

# 5 The fouling monitor

## 5.1 Selection of the measuring principle

At the start of the project for the development of a pilot monitor for gas-side fouling of heat exchangers, it had to be established which type of detection system should be considered for further research.
A number of criteria played an important role. A direct contact with the surface under examination must be avoided as far as possible. Besides that the monitor must be flexible because in general the gas-side surfaces of a heat exchanger are not easily accessible. The system must also not be too vulnerable because the monitor will often be used in aggressive environments.
Based on these considerations, non-contact methods like acoustic or optical detection systems are logical options.

The registration and/or generation of vibrations on surfaces of industrial heat exchangers is not likely to be easy. Gas and coolant streams of changing temperatures and the breaking off of pieces of fouling are potential important sources of interference for acoustic methods. Furthermore a solid contact must be made with the surface under examination for the registration of vibrations.

It was therefore decided to concentrate the research primarily on an optical system. Optical methods for the measurement of layer thickness, for example ellipsometry, have however not been considered because of the expected thickness and roughness of the layers. Thicknesses of several centimetres, the diversity of the fouling, from porous coal to cement-like materials and in some cases stalactites of many kilos, make reflective measurement of layer thicknesses impossible.

Deliberations with and earlier reports from the partners in the Joule project showed that there is a connection between the temperature distribution over the surface and the fouling of a heat exchanger. This can easily be explained by Figure 1. Figure 1[a] shows a drawing of a clean heat exchanger pipe and figure 1[b] shows a fouled heat exchanger pipe. The cold medium is inside the pipe and the hot medium (gas) is outside the tube. The temperature profile through the tube-wall can be drawn for both situations. In the figure it can easily be seen that a fouling layer results in a higher surface temperature. The fouling layer on the tube works like an isolating layer.

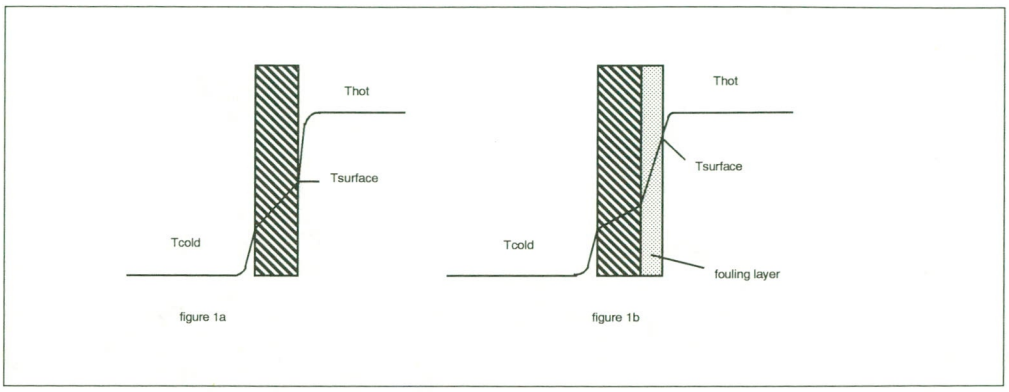


*Figure 1 Influence of fouling on the surface temperature*

The temperature of a surface is optically measurable by using the infra-red emission. Potential problems with this technique are the reflection of radiation by the surface under examination and the variable emissivity.
In addition the (changing) emission coefficient might give information on the nature of the fouling.

These considerations were the reason for concentrating efforts on the development of an image forming system for the registration of surface temperature and emissivity. This system uses a technique which is based on multi-wavelengths infra-red emission measurement.

## 5.2 Theoretical background

A literature search produced a number of articles in which infrared detection systems are described. The most useful was that of Tank and Dietl of the German "Institut für Optoelektronik" (1). It describes a method for the temperature measurement of highly reflective surfaces (patented in 1989).
The infrared radiation from a grey surface is determined by three parameters: surface temperature, environment radiation and emission coefficient. The principle of the technique described is the measurement of infrared energy at different wavelengths (theoretically at least three). After these measurements the three parameters can be determined from Planck's equations, by linearisation and consecutive fitting of these equations.

The Planck equation for the radiation intensity of a black body is given by:

$$B_\lambda = \frac{2hc^2}{\lambda^5\left(e^{\frac{hc}{\lambda kT}} - 1\right)}$$

Or the simplified Wien equation which may be used under the expected circumstances.

$$B_\lambda = \frac{2hc^2}{\lambda^5 e^{\frac{hc}{\lambda kT}}}$$

Where;

| | |
|---|---|
| h = Planck's constant | [Js] |
| c = speed of light | [m/s] |
| k = Boltzmann's constant | [J/K] |

A black body only exists in the laboratory but a so-called grey body is more common. The overall emission coefficient ($\varepsilon$) of a grey body ($\varepsilon<1$) is the ratio of the total emitted radiation of the grey body compared to that of a black surface ($\varepsilon=1$). Certain materials do not obey Planck's law. The emission coefficients can vary with the wavelength. Those materials are called selective radiators. Because the wavelengths used in this investigation are not too far apart, the emissivity of a surface is assumed to be wavelength independent. The emission coefficient also depends on the temperature. During one measurement the temperature has to be constant.
If the transmission coefficient is negligible one can derive::

$$r = 1 - \varepsilon$$

Here r is the reflection coefficient.
The emission coefficient is dependent on both the surface structure and the material properties. A rough surface generally results in a relatively low reflection coefficient and thus a high emission coefficient.

With measurements on a grey body the emission coefficient of the surface plays an important role but the temperature of the environment also has an influence. Especially in the case when the temperature of the environment is much higher compared to the temperature of the surface. Then the influence of the environment should also be taken into account. This leads to the following equation:

$$B_\lambda = \frac{2hc^2}{\lambda^5}\left(\frac{\varepsilon}{e^{\frac{hc}{\lambda kT_o}}} + \frac{1-\varepsilon}{e^{\frac{hc}{\lambda kT_e}}}\right)$$

Where;

| | | |
|---|---|---|
| B | = the measured radiation energy | [W/m$^2$] |
| h | = Planck's constant | [Js] |
| c | = speed of light | [m/s] |
| k | = Boltzmann's constant | [J/K] |
| $\lambda$ | = wavelength of the measurement | [m] |
| $\varepsilon$ | = emission coefficients | [-] |
| $T_o$ | = surface temperature | [K] |
| $T_e$ | = environment temperature | [K] |

In this equation $\varepsilon$, $T_o$ and $T_e$ are the parameters to be determined.

An example of the Planck curve can be seen in figure 2.
The equations can be solved using a non-linear curve-fitting iteration technique (Marquardt) on a computer.

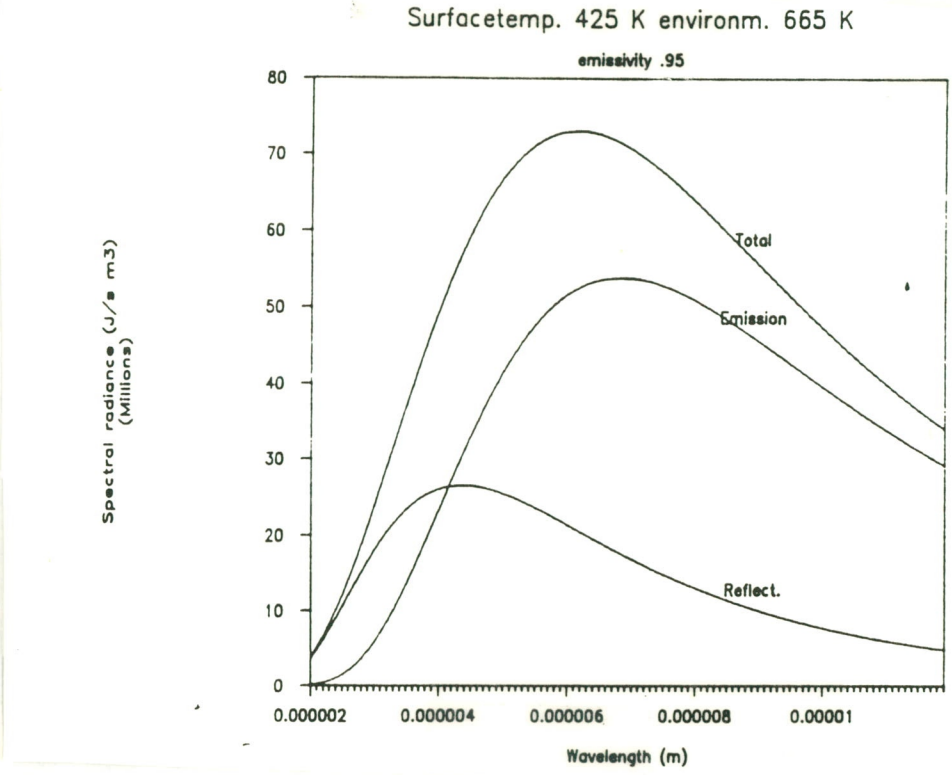


*Figure 2 Planck curve, emission and reflection*

## 5.3 The monitor

### 5.3.1 Introduction

Research was done on how to develop a fouling monitor with the emphasis on measurement of the gas-side surface temperatures of a heat exchanger. Moreover research was done on how to monitor the distribution over the surface of the temperature and the emission coefficient.
A technique which is developed is measurement of radiation at discrete wavelengths. To solve Planck's equation in theory measurements are needed at three wavelengths. To avoid the influence of gases, the discrete wavelengths should not be in the absorption peaks of the gases present (5.3.2).
The design of the monitor hardware, the choice of filters and the detector are described in 5.3.3.

The object temperature and the emission coefficient can be calculated from the infrared radiation emitted from the surface with the aid of an iterative computer program. The software needed for data collection, calculation of the conversion factors and the iterative software are described in 5.3.4.

### 5.3.2 Absorption of gasses

The preliminary tests were performed with a modified version of the so called gas cloud scanner from TNO [2]. This scanner is an instrument developed at TNO to meet the need to obtain greater insight into the spatial distribution of hazardous gases in work areas. With this scanner one can make IR-images of the distribution of a specific gas in space.
The scanner consists of an infrared emitter, a retro reflector screen, a scanning receiver and a filter system. To examine an indoor space the emitter and receiver are placed on one side of the space and a reflector screen on the other. Many gases and vapours have characteristic absorption peaks in the infrared part of the electromagnetic spectrum. By setting the receiver at the wavelength of this absorption-peak, the user can measure the amount in ppm*m of the specific gaseous component between receiver and reflector screen.
The filter wheel in the scanner can be set on wavelengths between 2.5 and 15.4 micrometer. After slight modifications, this made the scanner suitable for laboratory tests of the principle of the fouling monitor.

The problems encountered in these tests all relate to conversion of the data from the scanner into useable data for the calculation software.
The most important ones are the wavelength dependence of:
- the optical absorption of the atmosphere;
- the transmission of the filter wheel and the lenses;
- the sensitivity of the detector.

In order to find absorption-free windows in the spectrum suitable for the measurements and the correction factors needed for the calculations, scans were made over the spectrum using a near black body and a calibrated infrared source.
The scans gave a number of useable windows roughly between 3.5 and 9 μm, nicely spread over Planck's curve. In these windows a reliable result from the calculation software can be achieved.
These tests were executed in air. The absorption-free windows which were found are those free of absorption of gases which are common in air, like $CO_2$, $H_2O$ etc., see table 1. Gases which can exist in combustion outlets, like $SO_2$ and $NO_x$, were also taken in consideration in the selection of absorption-free windows (table 1).

*Table 1 Main absorption bands of combustion gases*

| | |
|---|---|
| Nitric Oxide | 5.2 μm |
| Nitrous Oxide | 4.4 μm |
| Carbon Dioxide | 2.7 μm |
| | 4.3 μm |
| Carbon Monoxide | 4.8 μm |
| Sulphor Dioxide | 4.1 μm |
| | 7.3 μm |
| Water | 4.8 μm |
| | 6.2 μm |

### 5.3.3 Design of the monitor

It proved very difficult to find a suitable detector which fulfils the spectral requirements obtained from the scanner tests.
Further calculations were therefore performed with the simulation software, using an extra window at approximately 2 μm. This window is only useful when measuring high temperatures. At higher temperatures the maximum of the Planck curve moves to lower wavelengths. The temperatures in industrial heat exchangers can be relatively high (600 °C), so there can be a sufficiently high level of infrared radiation at 2 μm.
The final choice for absorption-free windows expected to give satisfactory results were wavelengths between 2.1 - 2.4, 3.4 - 4.1 and 4.6 -4.8 μm.

For practical reasons the number of filters and the number of measurements at each filter must be kept to a minimum. This is because every measurement, together with the calculations, takes a fair amount of time. In addition the calculations have to be done for each pixel.
The simulation software was also used to find a satisfying number of filters and repetitions. This resulted in the choice of five narrow band filters ( 2.14, 2.275, 3.48, 3.64 and 4.7 μm) and 10 repetitions (number of measurements at one wavelength).

The advantage of using the region in the infrared spectrum between 2 and 5 μm is the availability of array detectors, which makes picture generation much easier.
With these restrictions in mind, the market was searched and the result was the purchase of a IRC-64 midwave infrared camera, made by Cincinnatti Electronics. This camera generates a picture of 64 x 64 pixels using an Indium Antimonide detector array without further filtering or signal processing, picture-generation excepted. More detailed information about of the IRC-64 camera is given in Appendix 1.

The developed calculations and signal processing can be performed with a PC and a framegrabber. Other additional hardware incorporated is a set of filters. The filters are controlled by the PC through a motorized filter wheel. A photograph of the camera and the filter wheel is shown in Appendix 2.

The camera has to be used in the corrected mode. It then corrects internally for the different responses of the pixels. This guarantees a uniform reaction of the different pixels.

Figure 3 shows the optical configuration of the monitor. This differs from the original configuration at two places. The original spectral filter in front of the InSb array is removed and a shiny aluminium pinhole replaces the adjustable iris. The iris is still part of the lens but has to be wide open all the time. The manufacturer advised replacement of an internal correction IC because of the pinhole.
An extra part in the optical configuration is of course the filter wheel. This is a keypad or computer controllable motorized filter wheel from ORIEL for five filters. A DC motor drives the filter wheel and Hall effect sensors detect what number filter is in position. The computer selects the filter number, filter interchange is 1 second for adjacent filters.

The filters used are manufactured by Spectrogon, Sweden. They are narrow band filters with a blocking from the ultraviolet to the far infrared. HW values are from 40 nm for the four shorter wavelength filters to 80 nm for the 4700 nm filter.

The calculations are rather time consuming in the set up with a normal PC, a dedicated chip could solve this problem at a later stage. Now the software only takes a streak 8 x 32 pixels from the picture under consideration.

The camera, framegrabber and filters together with a PC and conversion and iteration software form the monitor.

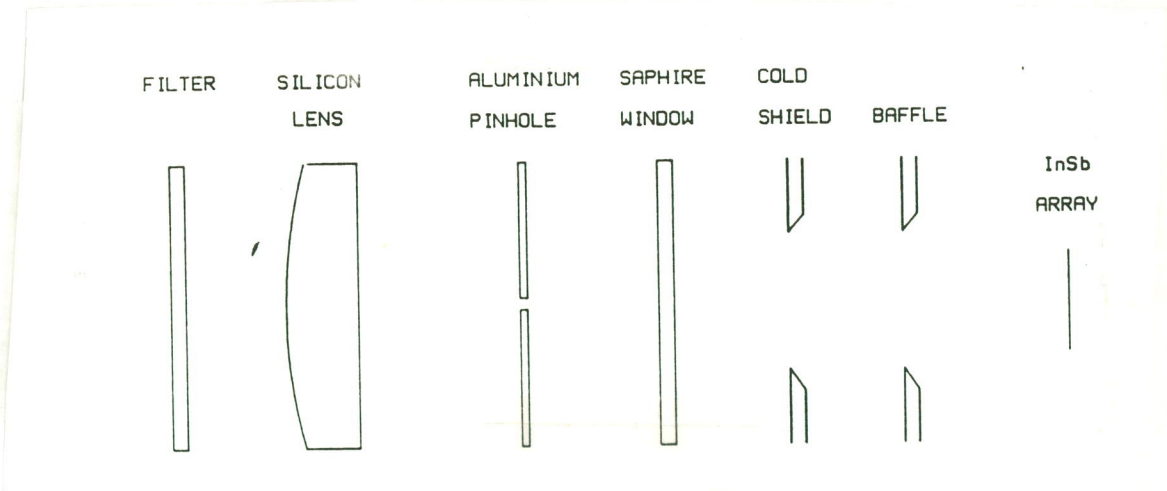


*Figure 3 Optical configuration of the camera*

### 5.3.4 Software

The software written for the camera consists of three parts:
1. Software which takes care of data acquisition.
2. Software which calculates the conversion constant and background radiation of the camera and software which converts binary data files into readable files for the curve fit program.
3. Iteration software which calculates the surface temperatures, reflection temperatures and emission coefficients.

1. The data collection software

Data collection with the monitor is performed under pre-set conditions and is separate from the calculations. The calculation software uses data files from the monitor created by this software.
The software takes care of the collection of data from the camera and controls the filterwheel. This software is written in C and compiled with "Microsoft C". The monitor was tested with the program "DATA10.EXE". This program instructs the camera to take 10 frames of 8x32 pixels in the centre of the picture at five different filter settings.
The DATA10.EXE program consists of four parts: the main body, a subroutine to instruct the board to take the specified number of 32K frames, a subroutine to read the collected data in user specified block sizes and a subroutine to set the filter positions.
In the main body the output file, the number of frames and the part of the picture to be examined is specified.

2. Software for calculation of background radiation and conversion factors

The correction factors and background radiation of the camera itself are needed to convert the values from the camera into corrected values for the intensity of the infrared radiation. These correction factors and background radiation are determined with aid of the PASCAL program CORBACK.PAS. The conversion factors correct for the different transparencies of the filters, and other aspects of the camera system. The data files used for calculation of the factors which are the result of calibration tests. The object for data collection in these tests is a black body at a known temperature.
When calculating the correction factors, the user can choose between two options: the first option is to determine the correction factor based on the measurement of one pixel. The second option is to determine the average correction factor from sixteen pixels situated in the middle of the image.
Using the temperature of the black body, the radiation at each of the five wavelengths used is calculated with Planck's formula. These calculations give the theoretical values for the radiation. Using the results of the calculations and the measurements with the camera, a correction factor is determined for each filter.
The camera's background radiation is the radiation of the camera itself on the detector. This is measured by placing a low emitting screen at room temperature just in front of the camera. The background values are determined by calculation of the average of the pixels.
The output of this program is a file with two sets of wavelength dependent numbers:

background corrections and conversion constants. This output file is needed for the program READRAW.

The purpose of the READRAW program is to convert the 5 binary data files as produced in the laboratory equipment into ASCII readable files for the curve fitting program. This program needs two input files, one input file with wavelength dependent background values and conversion constants, made with the programm CORBACK, and one file with data made by the data collection software.

3. The iteration software

The iteration software PIXELFIT is based on a non-linear curve fitting with Marquardt algorithm and developed by Dr. J.M. Reijn and L.A. Van der Hark of the Department of Computer Support of the Faculty of Pharmacy at Utrecht University, in collaboration with TNO.
The Marquardt algorithm [3] is a convenient algorithm which combines the best features of the gradient search with the method of linearizing. The fitting function can be obtained by increasing the diagonal terms of the curvature matrix by a factor which controls the interpolation of the algorithm between the two extremes.
This program needs the input file made by READRAW.

The software is tested with simulation software which created data with varying noise, wavelengths and temperatures.
During and after these tests the software was optimized and the required conditions for the measurements were set.

## 5.4 Practical monitor tests

### 5.4.1 Introduction

The second part of the project is to check the correctness of the calculated emission coefficient and surface temperatures. A test facility is therefore built up in which several surfaces are measured.
Afterwards the design of the camera is looked at. The most important question is whether the camera is suitable for use under industrial conditions.

### 5.4.2 Experimental set up

The testing of the fouling monitor is divided into 3 phases:
1. Experiments on a heated tube at room temperature;
2. Experiments on a cooled tube in a hot surrounding (in an oven);
3. Experiments on an industrial heat exchanger.

The first and second phases take place in the laboratory, the third phase of the experiments might take place at an industrial heat exchanger. The preparations have been made for the first two experiments and are described in this report.

The aim of the first two experiments is to test the principle of the method and to determine whether the temperatures and the emission coefficients measured and calculated by the monitor are in accordance with each other. The surface temperatures and emission coefficients are therefore being measured by alternative methods and the results of the two measurements will be compared.

The monitor is restricted because it can not measure accurately below a certain amount of radiation. When the temperature of the surface decreases the radiation from the surface will also decrease. So this will lead to a minimum temperature the monitor can measure.

### 5.4.3 Practical preparations

#### 5.4.3.1 Test tubes

The measurements are done on test tubes with different surfaces. For the first and second experimental phases fouled tube surfaces are created with different emission coefficients. The test tubes are fouled with the following materials:

1. Copa-slip: a mixture of lead, copper and bentone, a heat resistant paste used for protection of screws at high temperatures;
2. Black paint mixed with a sodium silicate solution;
3. Heat resistance mortal mixed with a sodium silicate solution;
4. Sable sand mixed with a sodium silicate solution fixed on fibrafax.

In the tubes a groove is made in which the thermocouples are adjusted. The surface thermocouples measure the temperature of the tube just under the surface of the fouling layer. The thermocouple is fixed just a little below the surface to be sure that we measure the surface temperature and not the temperature of the surrounding gas. The surface temperature as calculated by the monitor will be compared to the temperature measured by the thermocouples.

#### 5.4.3.2 Experiments on a heated tube at room temperature

Purpose: Measuring the relationship between the surface temperature and the emission coefficient of the surface.

The tube is attached between two clamps at a height of 1 m. The tubes are heated from the inside with a heating element. During the experiments the temperature is varied from 300 to 600 degrees Celsius. During the experiments the surface temperature is measured with a thermocouple.
When the temperature of the tube is varied the emission coefficient changes because it depends on the temperature. The emission coefficients are measured by two infrared cameras Cyclops 33, and AGA 780 working in different wavelength intervals (8-14μm and 3-5.6μm respectively). The cameras are placed perpendicular to the tube.

After these experiments the emission coefficients are known at various surface temperatures for the various tubes. This relationship will be used in the second experimental phase in a hot environment.

#### 5.4.3.3 Experiments in a hot surrounding

Purpose: Experimental determination of whether the monitor measures and calculates the correct emission coefficients and the right surface temperatures when it is in a hot environment.

The experiments take place in an electric tubular oven (Figure 4) into which the fouled tubes are inserted. The temperature of an inner alumina tube (inner diameter 10 cm, length 60 cm) can be varied over a temperature range from 25 to 1000 degrees Celsius.

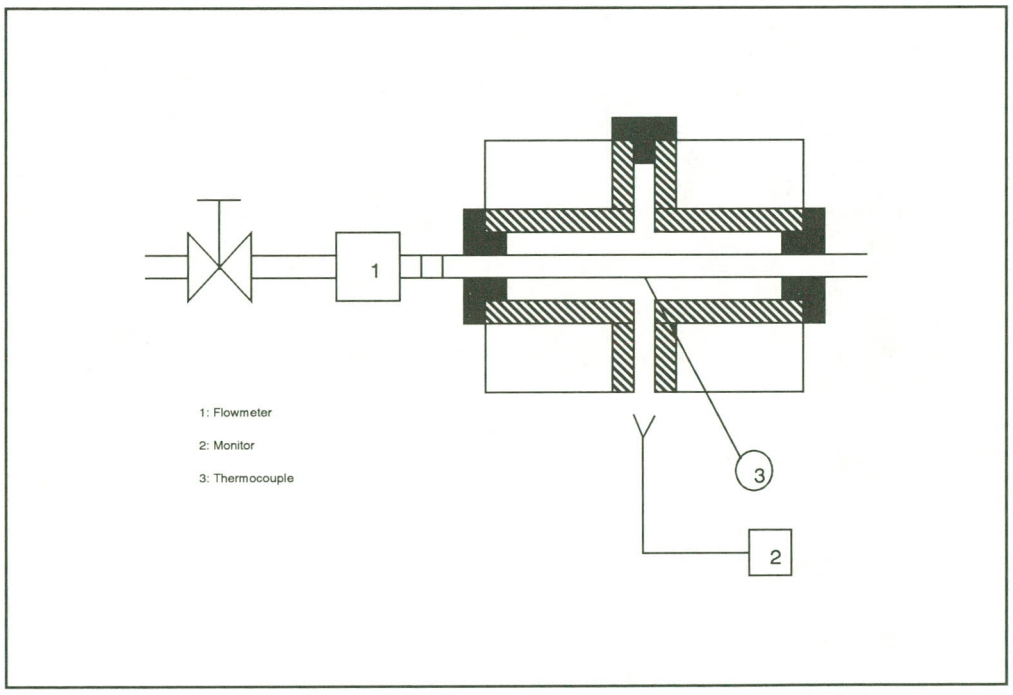


*Figure 4 Test facility cooled tube in oven*

The oven can be adjusted by three independent voltage sources. Each source regulates one part of the oven. Axial energy losses are reduced by thermal insulation of both ends. A hole (diameter 3.5 cm) in the side of the tubular oven permits monitoring of the test tube surfaces.
The tubes are placed in the oven and are cooled with an airstream from inside.
The surface temperature is measured by a thermocouple and is compared with the temperatures measured by the monitor.

In the first set of experiments the relationship was made between the emission coefficient of the surface and the surface temperature. These results can be used again to judge whether the emission coefficient determined by the monitor is correct.

The monitor is calibrated just before each measurement. A conical plug is placed in the oven. With the camera facing the plug, the plug appears as a black body. The correction factors are calculated with the CORBACK program.

### 5.4.4 Measuring Equipment

Thermocouples
The temperatures are measured with chromium alumal thermocouples.

Infrared cameras
The emission coefficient and the temperature of a surface can be measured by infrared detectors. At a known surface temperature and known ambient temperature the emission coefficient is derived from the equation:

$$\varepsilon = \frac{Q - \sigma T_e^4}{\sigma (T_0^4 - T_e^4)}$$

Where:

| | | |
|---|---|---|
| Q | : intensity of the radiation | [W/m$^2$] |
| $\sigma$ | : Stefan's constant | [W/m$^2$K$^4$] |

The temperature of the surface must be known when the emissivity of a surface is being measured. For these experiments two infrared cameras are available. More specifications of these cameras can be found in Appendix 1.

# 6 Results and discussion

## 6.1 Results

Final experiments have been done on only one tube: black paint mixed with a sodium silicate solution. Only one tube has been measured because the results of the first measurements showed large deviations. The method should first be improved before measurements on the other tubes are undertaken. Experiments are done at 5 different tubular oven temperatures. A set of measurements is made at each condition. The monitor measures the radiation of the surface and the object temperature, emission coefficient and reflection temperature of the environment are calculated with the curve fit program.
The results of the monitor experiments are listed in Appendix 3. Several recordings are made for one set of measurements at one temperature. Calculations have been made for three pixels for the different recordings. The results of these experiments are screened. Experiments with extreme results compared with the other experiments in the same set or which ended in a run-time error are ignored and rejected. The rejected experiments are marked with an asterisk(*) in Appendix 3.

The average of the object temperature, reflection temperature and emission coefficient will be determined for each set of measurements.
The formula used for this is:

$$X_{average} = \frac{1}{n}\sum X_i$$

X = parameter
n = number of measurements

The estimator of the variance of the experiments is also calculated. The root of the variance ($\sigma_{n-1}$) is an estimator of the average spread of the calculated temperatures or emission coefficients. For a good experiment this spread should be small. The formula used for the calculation of $\sigma_{n-1}$ is:

$$\sigma_{n-1} = \sqrt{\frac{1}{n-1}\sum (X_i - X_{average})^2}$$

The analysis of the results is broken down into three parts. In the first part the object temperature calculated by the monitor will be compared with the object temperature measured with the thermocouple (6.1.1). Because we intend to measure surface temperatures this parameter is the most important. Secondly the calculated emission coefficient will be compared with the measured emission coefficient (6.1.2) relating to the object temperature. And finally the reflection temperatures will be examined (6.1.3)

### 6.1.1 Comparison of the surface temperature

The surface temperature measured with the monitor (using the curve fit program) is compared with the temperature measured by a thermocouple attached to the surface.
The temperature of the surface measured by a thermocouple is listed in the first column of Table 2. The second column represents the number of measurements in that set of experiments, the third column represents the average of the calculated surface temperature and the fourth column represents the deviation of the object temperature, which is a degree of the spread in temperatures. The last columns represent the absolute and relative difference between the surface temperature measured by the thermocouple and the temperature measured by the monitor.

*Table 2 Surface temperatures ($T_o$)*

| Thermocouple measurement | Measurement with monitor | | | Comparison $T_{o,monitor}$ / $T_{o,thermocouple}$ | |
|---|---|---|---|---|---|
| $T_{o,thermo}$ [Kelvin] | n [-] | Average $T_{o,monitor}$ [Kelvin] | $\sigma_{n-1}$ [Kelvin] | Absolute difference [Kelvin] | Relative difference [%] |
| 639 | 17 | 653 | 7 | 14 | 2.1 |
| 683 | 12 | 690 | 17 | 7 | 1 |
| 712 | 15 | 687 | 21 | 25 | 3.5 |
| 738 | 4 | 727 | 12 | 11 | 1.4 |
| 807 | 8 | 720 | 44 | 87 | 10 |

It can be seen that the relative difference (column 6) between the thermocouple and monitor temperatures is less than 5 percent for the first, second, third and fourth set of experiments, which is quite good. From this standpoint it can be said that the monitor calculates the surface temperatures satisfactorily.
The average absolute fault in the measured temperature is 14 °C, in the first set of experiments and in the third set of experiments 25°C. Though the relative fault (column 6) between the temperature measured by the monitor and the temperature measured by the thermocouple is less than 5 percent, the absolute fault (column 5) in these sets of experiments is quite large.
The deviation (column 4) of the calculated surface temperature is quite large, especially for the second, third and fifth sets of experiments. This means the calculated surface temperature of the monitor has a wide spread. For a good experiment this spread should be smaller.
In summary: The calculation of the surface temperature is not satisfactory.

### 6.1.2 Comparison of the emissioncoefficient

The emission coefficient measured by the monitor is compared with the emission coefficient of a heated tube measured by the two infrared cameras.
The emission coefficient of a surface depends on the temperature of the surface. To determine the emission coefficient of a surface experiments are done at room temperature and the relationship between the surface temperature and the emission coefficient is measured separately with two infrared cameras. The results are listed in Table 3.

*Table 3 Relation between emission coefficient and surface temperature*

| Surface temperature [Kelvin] | Emission coefficient Cyclops | Emission coefficient AGA |
|---|---|---|
| 638 | 0.86 | 0.80 |
| 653 | 0.84 | |
| 731 | 0.87 | 0.80 |
| 744 | 0.84 | |
| 781 | 0.84 | |
| 807 | 0.87 | 0.80 |

From these results it is obvious that in this case measured emission coefficients hardly depend on the surface temperature. It can therefore be assumed that the emission coefficient is constant. The emission coefficient measured by the AGA and Cyclops were 0.80 and 0.86 respectively. These values are averaged in column three of Table 3. The inaccuracy of the measurement is 0.04, so the emission coefficient of the surface is 0.83 plus or minus 0.07. This emission coefficient (column four, Table 4) is used for comparison with the emission coefficient measured with the monitor.
The average of the emission coefficients and its deviation are determined from monitor measurements and are given in Table 4.

*Table 4 Emission coefficients (ε)*

| Monitor measurement | | | Measurement by two infrared cameras |
|---|---|---|---|
| n [-] | Average emission coefficient | $\sigma_{n-1}$ | Average emission coefficient |
| 17 | 0.958 | 0.017 | 0.83 |
| 12 | 0.735 | 0.053 | 0.83 |
| 15 | 0.75 | 0.14 | 0.83 |
| 4 | 0.75 | 0.038 | 0.83 |
| 8 | 0.54 | 0.2 | 0.83 |

It can be seen that the average emission coefficients of the second, third and fourth sets of experiments measured by the monitor are close to the emission coefficient determined by the infrared cameras. The fifth set of experiments shows an emission coefficient which is too low and the first set of experiments shows an emission coefficient which is too high.
The deviation ($\sigma_{n-1}$) of the third (0.14 or 19%) and fifth (0.2 or 37%) sets of experiments is very large, yet for a good experiment this spread should be small.
In summary, only the calculations of the emission coefficients in sets 2 and 4 are satisfactory. Sets 1, 2 and 5 of experiments have either a deviation or an absolute fault which is too large.

### 6.1.3 The reflection temperature

The reflection temperature itself, the average and the deviation are listed in Table 5 to give an impression of the reflection temperatures calculated by the monitor. Because it is very difficult to measure reflection temperatures separately, they can not be compared with other data.

Only the deviation of the reflection temperatures calculated by the monitor is examined.

*Table 5 Reflection temperatures ($T_r$)*

| Measurement monitor | | |
|---|---|---|
| Average $T_{calc}$ [Kelvin] | n [-] | $\sigma_{n-1}$ [Kelvin] |
| 1101 | 17 | 320 |
| 809 | 12 | 19 |
| 854 | 15 | 67 |
| 856 | 4 | 7.8 |
| 913 | 8 | 50 |

From Table 5 it can be seen that in particular the deviation of the first, third and fifth sets of experiments is large (more than 5%), which again is too large.

## 6.2 Discussion

***Results***

The differences between the object temperature and the emission coefficient measured by the monitor are in some cases relatively large compared with the separately measured temperature and emission coefficient. The deviation of the calculated parameters is also too large in most cases. This is probably caused by the following aspects:

1. The first aspect which is very important for the result of the surface temperature and emission coefficient calculated by the monitor is the quality of the dataset offered to the iteration program. During the experiments it became obvious that the response of the camera was not constant in time. This is probably caused by a loss of vacuum.

2. There is a large fluctuation in the raw data measured by the camera. This fluctuation in input data is sometimes more than 15 percent. These data are the input data for the iteration program. This fluctuation in input data will be relatively large for the lowest wavelength because then the absolute value of the radiation is small. This situation occurs during measurement at the smallest wavelengths (2.14 μm and 2.275) at low temperatures (T=650-700 K).
   A solution to this problem could be to base the datafit only on the three highest wavelengths during measurement at low temperatures. In addition the number of measurements at one wavelength can be raised, so the calculations will be more exact.
   A second solution to this problem could be to screen the raw data measured by the camera and to reject extreme data points.
   A third solution could be the use of another detector or another camera which is more sensitive and fluctuates less.
   Finally the probable loss of vacuum should be examined.

3. The results determined by the iterative software have a mathematical fault which in some cases is more than 30% for the calculated emission coefficient, more than 10% for the object temperature and more than 10 % for the reflection temperature. This poor convergence of the software can be caused by bad choices of initial estimators, by the fact that the iteration method is not suitable for solving that set of equations or it can be caused by the fluctuations in the input data of the iteration program.

The results of the measurements are still moderate, however, and it is expected that by improvement of the stability of the measuring method, the quality of the input data for the iteration program can be improved. This will probably result in more exact calculation of the surface temperatures and emission coefficients.

***Design of the Camera***

During the measurements the design of the camera is examined. During the experiments the following was revealed:
Because the monitor is a pilot model, there are still some weak points in the design of the monitor. The monitor is not yet suitable for use in environments with dust and aggressive components or water. Integrating the filters in the camera, for example, would make the system more robust. Another possibility is to place the camera in a box which is kept at a higher pressure than the environment. This protects the monitor against dust and harmful components.
The camera is cooled with liquid nitrogen. Another cooling system makes the camera easier to handle.

# 7 Economic assessment

—

# 8 Future work

Experiments showed that the response of the camera was not constant in time. There is a fluctuation in measuring data which, especially for the lower wavelength, is sometimes more than 15 percent. This fluctuation in input data is relatively large while the absolute values of the input data are small. The stability of the measuring method should therefore be improved.

The software consists of separate programs. The data collection and iteration software should be integrated.

In one run of the iteration software one pixel is calculated. The software should be adapted to calculate an array of pixels.

Integrating the filters in the camera would make the system more robust. A cooling system other than liquid nitrogen makes it easier to handle.

# 9 References

[1] V. Tank, H. Dietl,
Multispectral infrared pyrometer for temperature measurements with automatic correction of the influence of emissivity.
Infrared Phys. Vol. 30, No. 4. pp. 331- 342, 1990

[2] European patent,
EP 0 235 404 B1 3.
P.R. Bevington,
Data Reduction and Error Analysis for the Physical Sciences

*Generic studies for industrial heat exchanger fouling*
*Development of a Pilot-monitor*

## 10 Authentication

Name and address of the principal
The Commission of the European Communities
Directorate-General science
research and development
Brussels-Belgium

Names and functions of the cooperators
H.C. van Deventer -
S.I. Timmerman -
J.R. van der Vliet -

Names of establishments to which part of the research was put out to contract
Department of Compute Support
Faculty of Pharrmacy
Utrecht University

Date upon which, or period in which, the research took place
July 1990 - Jaunary 1993

Signature

Ir. S.I. Timmerman
research coordinator

Approved by

Ir. H.C. van Deventer
section leader

# Appendix 1 Technical Specifications

Specification of the camera (IRC-64):

| | |
|---|---|
| spectral respons: | 1-5.5 μm |
| detector: | Indium Antimode(IsSb) |
| number of elemnets: | 4096 (64*64) discrete detector elements |
| pixel pitch: | 100 μm |
| pixel size: | 55 μm |
| focus distance: | 3 feet to infinity |
| field of view: | 7.3 degrees * 7.3 degrees |
| resolution: | 2 * 2 milliradian |

Minolta/Land, type Cyclops 33, infrared spotmeter:

| | |
|---|---|
| — spectral respons: | 8 - 14 μm |
| — temperature range: | 0 - 100°C |
| — emission coefficient | 0.3 - 1.00 (minimal stepwidth 0.01) |
| — minimal spot size: | 13 mm at 0.75 m |

AGA Thermovision type 780, infrared camera:

| | |
|---|---|
| — spectral response: | 3 - 5.6 μm |
| — temperature range: | -20 - 850 °C |
| — emission coefficient: | 0.3 - 1.00 (minimal stepwidth 0.01) |

# Appendix 2 Photographs

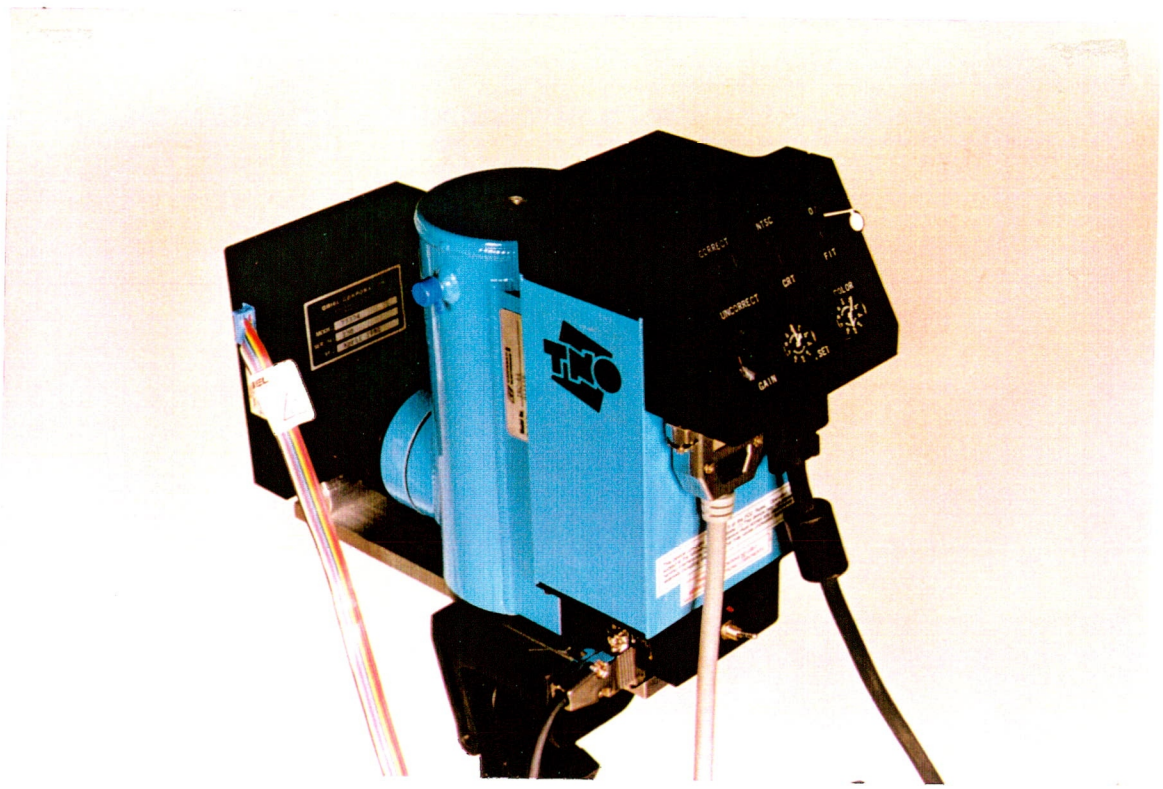


*Photograph 1 Monitor and filterwheel*

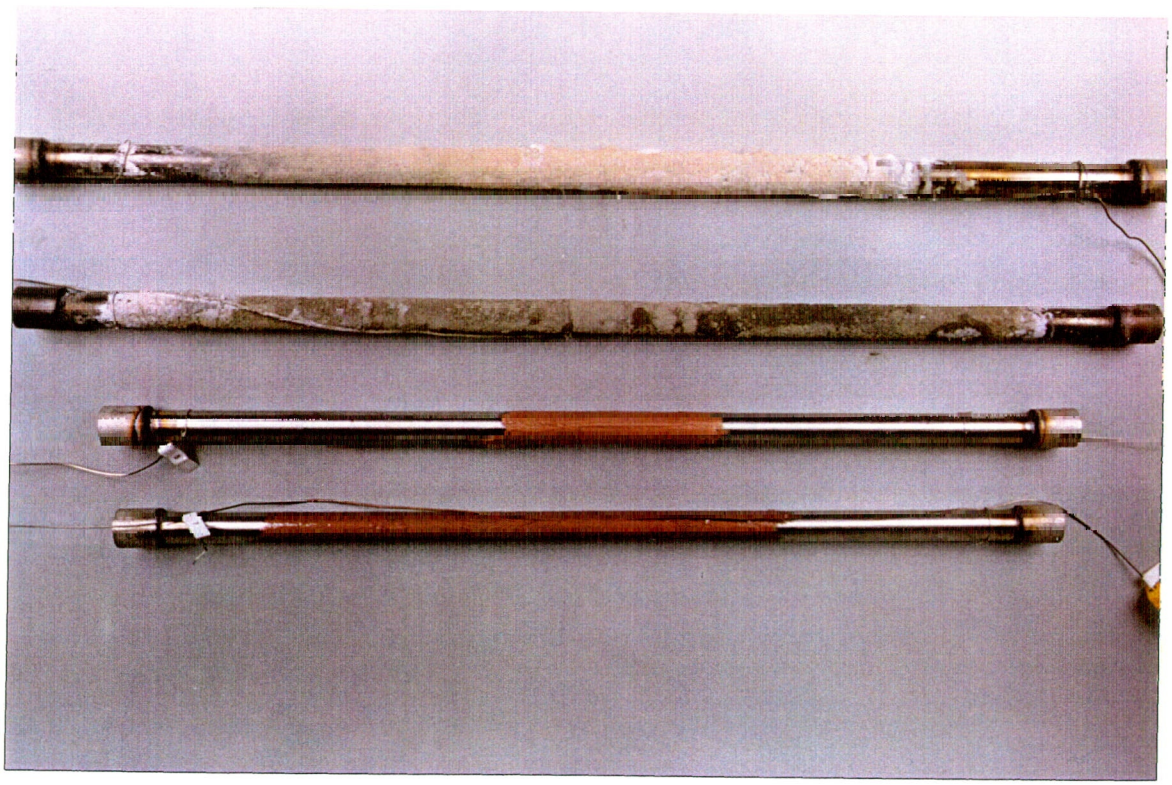

*Photograph 2 Fouled test tubes*

*Photograph 3 Tubular oven*

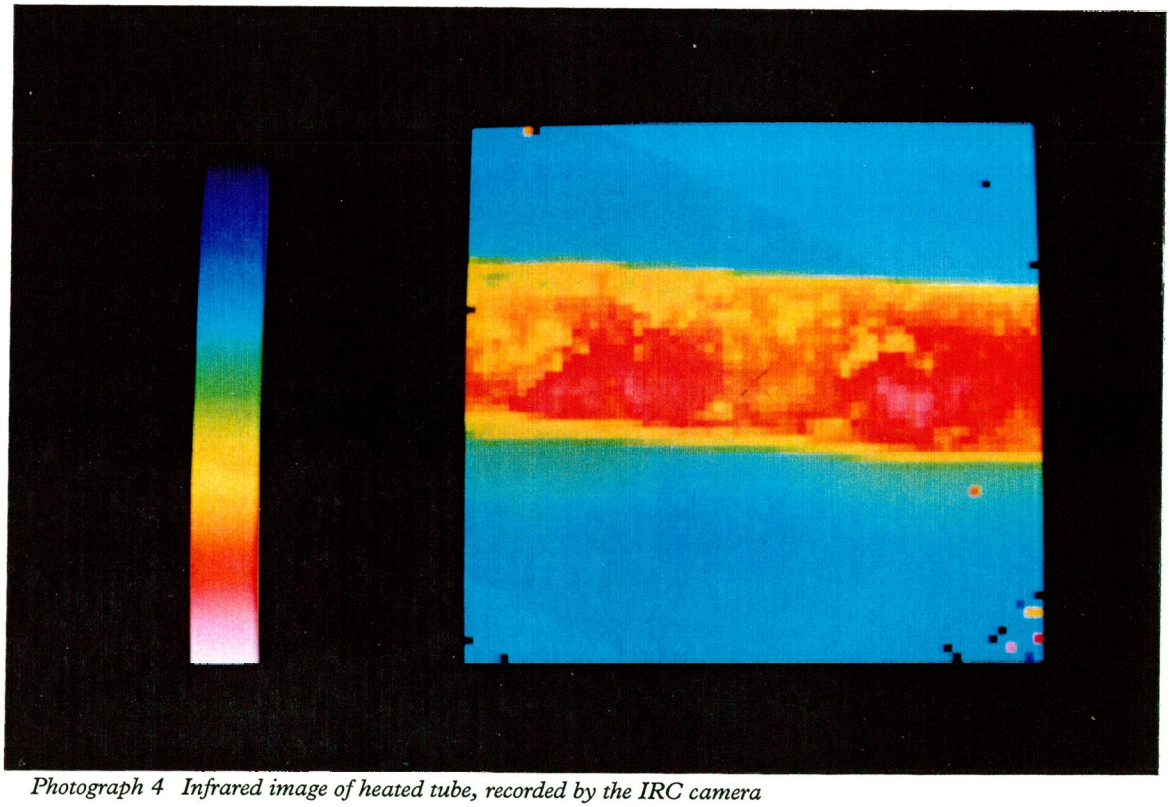

*Photograph 4 Infrared image of heated tube, recorded by the IRC camera*

# Appendix 3 Results of monitor calculations

The results of the calculations of the iterative programme are listed. The results are divided in 5 set of experiments. One set of experiments consists of the measurments at one temperature of the oven.
The name of the experiment is written down after 'data:'
The number of iterations tells how many iteration loops are done (maximum of 20).
The sum of squares "SSQ" is the value which is minimalised by the iterative programme and is given by the folowing formula:

$$SSQ = \sum_{i=1}^{n} (y_{data}(i) - y_{fit}(i))^2$$

The iterattive programme calculates the values and the mathematical faults for the emission coefficient(=epsilon), the surface temperature (object) and the reflection temperature (environment). The temperatures are in Kelvin.
The absulute value, the relative mathematical fault [%] and the absolute mathematical fault in the three parameters are listed for every experiment.

***Set experiments 1***

Results fit
data: 123.PIX, a367a23
Sum of squares 7.8565
Number of iterations: 20

| | | | | | |
|---|---|---|---|---|---|
| epsilon | 0.9625 | fault in %: | 4.9052 | absolute : | 0.0472 |
| object | 659.2125 | fault in %: | 1.2220 | absolute : | 8.0558 |
| environment | 897.4546 | fault in %: | 13.8357 | absolute : | 124.1688 |

Results fit
data: 132.PIX, a367a32
Sum of squares 3.8611
Number of iterations: 20

| | | | | | |
|---|---|---|---|---|---|
| epsilon | 0.9518 | fault in %: | 2.5443 | absolute : | 0.0242 |
| object | 647.5568 | fault in %: | 0.9791 | absolute : | 6.3400 |
| environment | 955.0687 | fault in %: | 6.3096 | absolute : | 60.2608 |

Results fit
data: 141.PIX, a367a41
Sum of squares 8.0209
Number of iterations: 20

| | | | | | |
|---|---|---|---|---|---|
| epsilon | 0.9674 | fault in %: | 1.3365 | absolute : | 0.0129 |
| object | 649.8945 | fault in %: | 0.6504 | absolute : | 4.2271 |
| environmnet | 1008.4536 | fault in %: | 5.3368 | absolute : | 53.8194 |

Results fit
data: 123.PIX, a367b23
Sum of squares 3.2208
Number of iterations: 20

| | | | | | |
|---|---|---|---|---|---|
| epsilon | 0.9554 | fault in %: | 2.2542 | absolute : | 0.0215 |
| object | 649.4895 | fault in % : | 0.8934 | absolute : | 5.8023 |
| environment | 960.6340 | fault in % : | 5.9665 | absolute : | 57.3160 |

Results fit
data: 132.PIX, a367b32
Sum of squares 4.2435
Number of iterations: 20

| | | | | | |
|---|---|---|---|---|---|
| epsilon | 0.9751 | fault in % : | 0.9435 | absolute : | 0.0092 |
| object | 651.1083 | fault in % : | 0.6014 | absolute : | 3.9159 |
| environment | 1076.2097 | fault in % : | 5.4326 | absolute : | 58.4666 |

Results fit
data: 141.PIX, a367b41
Sum of squares 3.7756
Number of iterations: 20

| | | | | | |
|---|---|---|---|---|---|
| epsilon | 0.9600 | fault in %: | 1.9933 | absolute : | 0.0191 |
| object | 650.3785 | fault in %: | 0.8376 | absolute : | 5.4476 |
| environment | 981.7848 | fault in %: | 6.1987 | absolute : | 60.8582 |

Results fit
data: 123.PIX, a367c23
Sum of squares 2.3641
Number of iterations: 20

| | | | | | |
|---|---|---|---|---|---|
| epsilon | 0.9428 | fault in %: | 3.0072 | absolute : | 0.0284 |
| object | 645.8168 | fault in %: | 1.1057 | absolute : | 7.1405 |
| environment | 940.9988 | fault in %: | 6.0636 | absolute : | 57.0583 |

Results fit
data: 132.PIX, a367c32
Sum of squares 2.3061
Number of iterations: 20

| | | | | | |
|---|---|---|---|---|---|
| epsilon | 0.9397 | fault in %: | 2.6768 | absolute : | 0.0252 |
| object | 642.2467 | fault in %: | 1.0850 | absolute : | 6.9684 |
| environment | 952.7954 | fault in %: | 5.1792 | absolute : | 49.3470 |

Results fit
data: 141.PIX, a367c41
Sum of squares 3.3607
Number of iterations: 20

| | | | | | |
|---|---|---|---|---|---|
| epsilon | 0.9709 | fault in %: | 1.2580 | absolute : | 0.0122 |
| object | 650.7289 | fault in %: | 0.7110 | absolute : | 4.6267 |
| environment | 1044.5332 | fault in %: | 5.9845 | absolute : | 62.5100 |

**Results fit
data: 123.PIX, b367a23
Sum of squares 10.4116
Number of iterations: 8

| | | | | | |
|---|---|---|---|---|---|
| epsilon | 0.8827 | fault in %: | ********** | absolute : | 9528.0128 |
| object | 670.7471 | fault in %: | 3370.9558 | absolute : | ********** |
| environment | 674.9101 | fault in %: | ********** | absolute : | ********** |

Results fit
data: 132.PIX, b367a32
Sum of squares 4.9211
Number of iterations: 20

| | | | | | |
|---|---|---|---|---|---|
| epsilon | 0.9570 | fault in %: | 3.7586 | absolute : | 0.0360 |
| object | 652.7383 | fault in %: | 1.1841 | absolute : | 7.7293 |
| environment | 920.0651 | fault in %: | 9.5131 | absolute : | 87.5271 |

Results fit
data: 141.PIX, b367a41
Sum of squares 8.8882
Number of iterations: 20

| | | | | | |
|---|---|---|---|---|---|
| epsilon | 0.9987 | fault in %: | 0.1003 | absolute : | 0.0010 |
| object | 665.3347 | fault in %: | 0.2006 | absolute : | 1.3346 |
| environment | 1654.1522 | fault in %: | 18.5602 | absolute : | 307.0136 |

Results fit
data: 123.PIX, b367b23
Sum of squares 4.0219
Number of iterations: 20

| | | | | | |
|---|---|---|---|---|---|
| epsilon | 0.9496 | fault in %: | 4.2306 | absolute : | 0.0402 |
| object | 651.9534 | fault in %: | 1.2477 | absolute : | 8.1346 |
| environment | 903.0414 | fault in %: | 8.5825 | absolute : | 77.5038 |

Results fit
data: 132.PIX, b367b32
Sum of squares 4.0153
Number of iterations: 20

| | | | | | |
|---|---|---|---|---|---|
| epsilon | 0.9990 | fault in %: | 0.0704 | absolute : | 0.0007 |
| object | 666.3504 | fault in %: | 0.2080 | absolute : | 1.3859 |
| environment | 1931.5235 | fault in %: | 20.5058 | absolute : | 396.0742 |

Results fit
data: 141.PIX, b367b41
Sum of squares 4.8082
Number of iterations: 20

| | | | | | |
|---|---|---|---|---|---|
| epsilon | 0.9355 | fault in %: | 5.5307 | absolute : | 0.0517 |
| object | 649.3123 | fault in %: | 1.4653 | absolute : | 9.5146 |
| environment | 883.7334 | fault in %: | 8.3801 | absolute : | 74.0580 |

Results fit
data: 123.PIX, b367c23
Sum of squares 2.7202
Number of iterations: 20

| | | | | | |
|---|---|---|---|---|---|
| epsilon | 0.9455 | fault in %: | 4.6043 | absolute : | 0.0435 |
| object | 650.8154 | fault in %: | 1.3594 | absolute : | 8.8472 |
| environment | 903.4916 | fault in %: | 8.7806 | absolute : | 79.3318 |

Results fit
data: 132.PIX, b367c32
Sum of squares 2.3931
Number of iterations: 20

| | | | | | |
|---|---|---|---|---|---|
| epsilon | 0.9632 | fault in %: | 2.3751 | absolute : | 0.0229 |
| object | 652.3623 | fault in %: | 0.9678 | absolute : | 6.3133 |
| environment | 970.0963 | fault in %: | 7.7262 | absolute : | 74.9515 |

Results fit
data: 141.PIX, b367c41
Sum of squares 2.9525
Number of iterations: 20

| | | | | | |
|---|---|---|---|---|---|
| epsilon | 0.9987 | fault in %: | 0.1020 | absolute : | 0.0010 |
| object | 666.2716 | fault in %: | 0.2414 | absolute : | 1.6086 |
| environment | 1746.3790 | fault in %: | 19.7786 | absolute : | 345.4097 |

***Set experiments 2***

Results fit
data: 123.PIX, a410a23
Sum of squares 1.4223
Number of iterations: 3

| | | | | | |
|---|---|---|---|---|---|
| epsilon | 0.7279 | fault in %: | 114.8409 | absolute : | 0.8360 |
| object | 704.1856 | fault in %: | 8.7259 | absolute : | 61.4466 |
| environment | 796.5619 | fault in %: | 15.7646 | absolute : | 125.5750 |

Results fit
data: 132.PIX, a410a32
Sum of squares 2.1975
Number of iterations: 4

| | | | | | |
|---|---|---|---|---|---|
| epsilon | 0.7296 | fault in %: | 46.6457 | absolute : | 0.3403 |
| object | 685.3369 | fault in %: | 5.3079 | absolute : | 36.3772 |
| environment | 813.0948 | fault in %: | 8.4779 | absolute : | 68.9335 |

Results fit
data: 141.PIX, a410a41
Sum of squares 1.9075
Number of iterations: 4

| | | | | | |
|---|---|---|---|---|---|
| epsilon | 0.6751 | fault in %: | 41.2546 | absolute : | 0.2785 |
| object | 667.1899 | fault in %: | 5.6569 | absolute : | 37.7424 |
| environment | 811.1122 | fault in %: | 6.3953 | absolute : | 51.8733 |

Results fit
data: 123.PIX, a410b23
Sum of squares 1.6664
Number of iterations: 5

| | | | | | |
|---|---|---|---|---|---|
| epsilon | 0.8062 | fault in %: | 85.9036 | absolute : | 0.6926 |
| object | 709.7099 | fault in %: | 7.1238 | absolute : | 50.5581 |
| environment | 810.8040 | fault in %: | 19.7003 | absolute : | 159.7310 |

Results fit
data: 132.PIX, a410b32
Sum of squares 1.1967
Number of iterations: 4

| | | | | | |
|---|---|---|---|---|---|
| epsilon | 0.8206 | fault in %: | 27.3202 | absolute : | 0.2242 |
| object | 690.2353 | fault in %: | 4.0476 | absolute : | 27.9382 |
| environment | 848.9736 | fault in %: | 9.6392 | absolute : | 81.8342 |

Results fit
data: 141.PIX, a410b41
Sum of squares 1.0786
Number of iterations: 3

| | | | | | |
|---|---|---|---|---|---|
| epsilon | 0.7292 | fault in %: | 29.4734 | absolute : | 0.2149 |
| object | 670.5513 | fault in %: | 4.4820 | absolute : | 30.0540 |
| environment | 827.1340 | fault in %: | 6.2102 | absolute : | 51.3671 |

Results fit
data: 123.PIX, b410a23
Sum of squares 1.0880
Number of iterations: 4

| | | | | | |
|---|---|---|---|---|---|
| epsilon | 0.7167 | fault in %: | 429.3010 | absolute : | 3.0770 |
| object | 713.5562 | fault in %: | 19.6712 | absolute : | 140.3653 |
| environment | 773.0577 | fault in %: | 38.4445 | absolute : | 297.1981 |

Results fit
data: 132.PIX, b410a32
Sum of squares 1.6536
Number of iterations: 4

| | | | | | |
|---|---|---|---|---|---|
| epsilon | 0.7264 | fault in %: | 72.1708 | absolute : | 0.5242 |
| object | 690.6177 | fault in %: | 6.8251 | absolute : | 47.1355 |
| environment | 800.6030 | fault in %: | 11.4700 | absolute : | 91.8291 |

Results fit
data: 141.PIX, b410a41
Sum of squares 1.5516
Number of iterations: 4

| | | | | | |
|---|---|---|---|---|---|
| epsilon | 0.6540 | fault in %: | 61.5156 | absolute : | 0.4023 |
| object | 671.0976 | fault in %: | 7.2096 | absolute : | 48.3833 |
| environment | 798.1487 | fault in %: | 7.8821 | absolute : | 62.9111 |

Results fit
data: 123.PIX, b410b23
Sum of squares 1.3286
Number of iterations: 4

| | | | | | |
|---|---|---|---|---|---|
| epsilon | 0.7782 | fault in %: | 220.2723 | absolute : | 1.7142 |
| object | 713.4258 | fault in % : | 12.8664 | absolute : | 91.7922 |
| environment | 787.8457 | fault in %: | 33.1394 | absolute : | 261.0876 |

Results fit
data: 132.PIX, b410b32
Sum of squares 1.1661
Number of iterations: 4

| | | | | | |
|---|---|---|---|---|---|
| epsilon | 0.8137 | fault in %: | 40.1158 | absolute : | 0.3264 |
| object | 693.3238 | fault in %: | 5.0707 | absolute : | 35.1567 |
| environment | 833.1601 | fault in %: | 12.3198 | absolute : | 102.6437 |

Results fit
data: 141.PIX, b410b41
Sum of squares 1.1616
Number of iterations: 3

| | | | | | |
|---|---|---|---|---|---|
| epsilon | 0.7188 | fault in %: | 41.2013 | absolute : | 0.2962 |
| object | 674.3892 | fault in %: | 5.4501 | absolute : | 36.7551 |
| environment | 814.9821 | fault in %: | 7.6054 | absolute : | 61.9829 |

***Set experiment 3***

Results fit
data: 123.PIX, a439a23
Sum of squares 3.5949
Number of iterations: 4

| | | | | | |
|---|---|---|---|---|---|
| epsilon | 0.6975 | fault in %: | 32.8017 | absolute : | 0.2288 |
| object | 678.0018 | fault in %: | 4.7249 | absolute : | 32.0348 |
| environment | 830.6932 | fault in %: | 5.8051 | absolute : | 48.2226 |

**Results fit
data: 132.PIX, a439a32
Sum of squares 6.4900
Number of iterations: 20

| | | | | | |
|---|---|---|---|---|---|
| epsilon | 0.2948 | fault in %: | 16.2949 | absolute : | 0.0480 |
| object | 539.6372 | fault in %: | 6.6578 | absolute : | 35.9281 |
| environment | 782.7390 | fault in %: | 0.7708 | absolute : | 6.0335 |

Results fit
data: 141.PIX, a439a41
Sum of squares 6.1208
Number of iterations: 4

| | | | | | |
|---|---|---|---|---|---|
| epsilon | 0.7308 | fault in %: | 24.0329 | absolute : | 0.1756 |
| object | 677.2101 | fault in %: | 3.7717 | absolute : | 25.5421 |
| environment | 840.9826 | fault in %: | 5.2815 | absolute : | 44.4166 |

Results fit
data: 123.PIX, a439b23
Sum of squares 1.4451
Number of iterations: 4

| | | | | | |
|---|---|---|---|---|---|
| epsilon | 0.7682 | fault in %: | 31.1208 | absolute : | 0.2391 |
| object | 690.2126 | fault in %: | 4.3821 | absolute : | 30.2460 |
| environment | 842.6723 | fault in %: | 7.7804 | absolute : | 65.5637 |

Results fit
data: 132.PIX, a439b32
Sum of squares 1.5460
Number of iterations: 4

| | | | | | |
|---|---|---|---|---|---|
| epsilon | 0.7553 | fault in %: | 21.8736 | absolute : | 0.1652 |
| object | 678.5373 | fault in %: | 3.8013 | absolute : | 25.7930 |
| environment | 855.6930 | fault in %: | 5.6950 | absolute : | 48.7316 |

Results fit
data: 141.PIX. a439b41
Sum of squares 3.5540
Number of iterations: 4

| | | | | | |
|---|---|---|---|---|---|
| epsilon | 0.7753 | fault in %: | 21.5772 | absolute : | 0.1673 |
| object | 686.4352 | fault in %: | 3.2416 | absolute : | 22.2515 |
| environment | 845.9165 | fault in %: | 5.8422 | absolute : | 49.4199 |

Results fit
data: 123.PIX, a439c23
Sum of squares 2.7463
Number of iterations: 11

| | | | | | |
|---|---|---|---|---|---|
| epsilon | 0.9511 | fault in %: | 8.8134 | absolute : | 0.0838 |
| object | 721.2870 | fault in %: | 1.7826 | absolute : | 12.8580 |
| environment | 940.2666 | fault in %: | 16.4281 | absolute : | 154.4683 |

Results fit
data: 132.PIX, a439c32
Sum of squares 1.4404
Number of iterations: 20

| | | | | | |
|---|---|---|---|---|---|
| epsilon | 0.9036 | fault in %: | 7.0718 | absolute : | 0.0639 |
| object | 700.9705 | fault in %: | 1.5370 | absolute : | 10.7736 |
| environment | 922.2137 | fault in %: | 6.4041 | absolute : | 59.0594 |

Results fit
data: 141.PIX, a439c41
Sum of squares 2.3014
Number of iterations: 20

| | | | | | |
|---|---|---|---|---|---|
| epsilon | 0.9730 | fault in %: | 1.8191 | absolute : | 0.0177 |
| object | 710.2150 | fault in %: | 0.7052 | absolute : | 5.0083 |
| environment | 1054.9404 | fault in %: | 8.5043 | absolute : | 89.7149 |

**results fit
data: 123.PIX, b439a23
Sum of squares 4.9469
Number of iterations: 20

| | | | | | |
|---|---|---|---|---|---|
| epsilon | 0.2686 | fault in %: | 65.2092 | absolute : | 0.1752 |
| object | 600.6774 | fault in %: | 12.9377 | absolute : | 77.7137 |
| environment | 767.9902 | fault in %: | 2.0548 | absolute : | 15.7806 |

**results fit
data: 132.PIX, b439a32
Sum of squares 9.8417
Number of iterations: 20

| | | | | | |
|---|---|---|---|---|---|
| epsilon | 0.1995 | fault in %: | 14.1600 | absolute : | 0.0282 |
| object | 463.8520 | fault in %: | 12.4482 | absolute : | 57.7413 |
| environment | 767.5635 | fault in %: | 0.4633 | absolute : | 3.5561 |

Results fit
data: 141.PIX, b439a41
Sum of squares 7.2872
Number of iterations: 20

| | | | | | |
|---|---|---|---|---|---|
| epsilon | 0.3835 | fault in %: | 56.7296 | absolute : | 0.2176 |
| object | 626.4893 | fault in %: | 9.2634 | absolute : | 58.0344 |
| environment | 779.2221 | fault in %: | 2.8194 | absolute : | 21.9694 |

Results fit
data: 123.PIX, b439b23
Sum of squares 1.6701
Number of iterations: 3

| | | | | | |
|---|---|---|---|---|---|
| epsilon | 0.6836 | fault in %: | 82.4721 | absolute : | 0.5638 |
| object | 691.4822 | fault in %: | 8.1807 | absolute : | 56.5684 |
| environment | 805.2101 | fault in %: | 10.8274 | absolute : | 87.1834 |

Results fit
data: 132.PIX, b439b32
Sum of squares 2.0762
Number of iterations: 4

| | | | | | |
|---|---|---|---|---|---|
| epsilon | 0.6800 | fault in %: | 44.1722 | absolute : | 0.3004 |
| object | 677.6001 | fault in %: | 5.9635 | absolute : | 40.4083 |
| environment | 821.5039 | fault in %: | 6.8522 | absolute : | 56.2914 |

Results fit
data: 141.PIX, b439b41
Sum of squares 3.7494
Number of iterations: 3

| | | | | | |
|---|---|---|---|---|---|
| epsilon | 0.6732 | fault in %: | 54.0872 | absolute : | 0.3641 |
| object | 684.5178 | fault in %: | 5.9097 | absolute : | 40.4531 |
| environment | 806.4753 | fault in %: | 7.2032 | absolute : | 58.0921 |

Results fit
data: 123.PIX, b439c23
Sum of squares 1.5603
Number of iterations: 4

| | | | | | |
|---|---|---|---|---|---|
| epsilon | 0.8043 | fault in %: | 103.6199 | absolute : | 0.8334 |
| object | 713.1093 | fault in %: | 8.4193 | absolute : | 60.0387 |
| environment | 813.0636 | fault in %: | 23.1843 | absolute : | 188.5033 |

Results fit
data: 132.PIX, b439c32
Sum of squares 1.3445
Number of iterations: 4

| | | | | | |
|---|---|---|---|---|---|
| epsilon | 0.7319 | fault in %: | 31.9829 | absolute : | 0.2341 |
| object | 684.6352 | fault in %: | 4.1345 | absolute : | 28.3063 |
| environment | 825.3415 | fault in %: | 6.2464 | absolute : | 51.5538 |

Results fit
data: 141.PIX, b439c41
Sum of squares 2.1573
Number of iterations: 5

| | | | | | |
|---|---|---|---|---|---|
| epsilon | 0.7938 | fault in %: | 24.0035 | absolute : | 0.1905 |
| object | 687.8479 | fault in %: | 3.2812 | absolute : | 22.5697 |
| environment | 837.2919 | fault in %: | 7.0369 | absolute : | 58.9196 |

***Set experiments 4***

**results fit
data: 123.PIX, a465a23
Sum of squares 8.9128
Number of iterations: 13

| | | | | | | |
|---|---|---|---|---|---|---|
| epsilon | 0.9517 | fault in % : | ********** | absolute | : | 1838.2544 |
| object | 772.0187 | fault in % : | 918.2166 | absolute | : | 7088.8044 |
| environment | 764.6085 | fault in % : | ********** | absolute | : | ********** |

Results fit
data: 132.PIX, a465a32
Sum of squares 2.1145
Number of iterations: 5

| | | | | | | |
|---|---|---|---|---|---|---|
| epsilon | 0.7915 | fault in % : | 64.5317 | absolute | : | 0.5108 |
| object | 738.2016 | fault in % : | 5.7870 | absolute | : | 42.7194 |
| environment | 852.2461 | fault in % : | 14.5419 | absolute | : | 123.9324 |

Results fit
data: 141.PIX, a465a41
Sum of squares 2.2567
Number of iterations: 5

| | | | | | | |
|---|---|---|---|---|---|---|
| epsilon | 0.7636 | fault in % : | 30.3981 | absolute | : | 0.2321 |
| object | 720.2849 | fault in % : | 3.9175 | absolute | : | 28.2171 |
| environment | 869.8091 | fault in % : | 7.2242 | absolute | : | 62.8372 |

**Results fit
data: 123.PIX, b465a23
Sum of squares 8.9380
Number of iterations: 11

| | | | | | | |
|---|---|---|---|---|---|---|
| epsilon | 0.9465 | fault in % : | ********** | absolute | : | 943.0529 |
| object | 773.1302 | fault in % : | 586.8929 | absolute | : | 4537.4467 |
| environment | 763.9166 | fault in % : | ********** | absolute | : | ********** |

Results fit
data: 132.PIX, b465a32
Sum of squares 2.1855
Number of iterations: 5

| | | | | | | |
|---|---|---|---|---|---|---|
| epsilon | 0.7734 | fault in % : | 72.3116 | absolute | : | 0.5593 |
| object | 737.6421 | fault in % : | 6.2605 | absolute | : | 46.1800 |
| environment | 848.0801 | fault in % : | 14.2904 | absolute | : | 121.1941 |

Results fit
data: 141.PIX, b465a41
Sum of squares 1.3138
Number of iterations: 4

| | | | | | | |
|---|---|---|---|---|---|---|
| epsilon | 0.7079 | fault in % : | 39.2014 | absolute | : | 0.2775 |
| object | 714.7029 | fault in % : | 4.8389 | absolute | : | 34.5841 |
| environment | 857.7151 | fault in % : | 6.7888 | absolute | : | 58.2286 |

***Set experiments 5***

**Results fit
data: 123.PIX, a534a23
Sum of squares 21.4707
Number of iterations: 20

| | | | | | |
|---|---|---|---|---|---|
| epsilon | 0.1644 | fault in %: | 15.6511 | absolute : | 0.0257 |
| object | 543.8325 | fault in %: | 9.2528 | absolute : | 50.3195 |
| environment | 852.4487 | fault in %: | 0.3845 | absolute : | 3.2776 |

**Results fit
data:132.pix, a534a32: runtime error

**Results fit
data:141.pix, a534a41: runtime error

Results fit
data: 123.PIX, a534b23
Sum of squares 2.5623
Number of iterations: 20

| | | | | | |
|---|---|---|---|---|---|
| epsilon | 0.3358 | fault in %: | 62.4466 | absolute : | 0.2097 |
| object | 691.6608 | fault in %: | 10.5799 | absolute : | 73.1767 |
| environment | 869.7894 | fault in %: | 2.6482 | absolute : | 23.0341 |

Results fit
data: 132.PIX, a534b32
Sum of squares 2.3122
Number of iterations: 20

| | | | | | |
|---|---|---|---|---|---|
| epsilon | 0.3135 | fault in %: | 27.5233 | absolute : | 0.0863 |
| object | 660.4013 | fault in %: | 6.2413 | absolute : | 41.2178 |
| environment | 871.0205 | fault in %: | 1.2124 | absolute : | 10.5606 |

Results fit
data: 141.PIX, a534b41
Sum of squares 1.6897
Number of iterations: 20

| | | | | | |
|---|---|---|---|---|---|
| epsilon | 0.3367 | fault in %: | 29.8633 | absolute : | 0.1006 |
| object | 666.1840 | fault in %: | 6.3521 | absolute : | 42.3168 |
| environment | 867.8793 | fault in %: | 1.4039 | absolute : | 12.1840 |

**Results fit
data: 123.PIX, b534a23
Sum of squares*********
Number of iterations: 20

| | | | | | |
|---|---|---|---|---|---|
| epsilon | 0.7790 | fault in %: | 0.5661 | absolute : | 0.0044 |
| object | 635.1952 | fault in %: | 0.5227 | absolute : | 3.3202 |
| environment | 1204.6799 | fault in %: | 0.3486 | absolute : | 4.1998 |

Results fit
data: 132.PIX, b534a32
Sum of squares 16.7466
Number of iterations: 6

| | | | | | |
|---|---|---|---|---|---|
| epsilon | 0.6497 | fault in %: | 22.0910 | absolute : | 0.1435 |
| object | 750.3536 | fault in %: | 3.0381 | absolute : | 22.7967 |
| environment | 918.0098 | fault in %: | 3.2219 | absolute : | 29.5774 |

Results fit
data: 141.PIX, b534a41
Sum of squares 12.0183
Number of iterations: 20

| | | | | | |
|---|---|---|---|---|---|
| epsilon | 0.9086 | fault in %: | 6.0261 | absolute : | 0.0548 |
| object | 782.5816 | fault in %: | 1.2441 | absolute : | 9.7358 |
| environment | 1032.1955 | fault in %: | 6.0802 | absolute : | 62.7596 |

Results fit
data: 123.PIX, b534b23
Sum of squares 5.0327
Number of iterations: 5

| | | | | | |
|---|---|---|---|---|---|
| epsilon | 0.6278 | fault in %: | 42.4951 | absolute : | 0.2668 |
| object | 750.2398 | fault in %: | 5.8045 | absolute : | 43.5475 |
| environment | 916.6000 | fault in %: | 5.5541 | absolute : | 50.9088 |

Results fit
data: 132.PIX. b534b32
Sum of squares 4.3142
Number of iterations: 6

| | | | | | |
|---|---|---|---|---|---|
| epsilon | 0.5737 | fault in %: | 20.5935 | absolute : | 0.1181 |
| object | 729.8557 | fault in %: | 3.3568 | absolute : | 24.4999 |
| environment | 914.3843 | fault in %: | 2.3539 | absolute : | 21.5234 |

Results fit
data: 141.PIX, b534b41
Sum of squares 8.9810
Number of iterations: 5

| | | | | | |
|---|---|---|---|---|---|
| epsilon | 0.6341 | fault in %: | 25.6050 | absolute : | 0.1624 |
| object | 735.3388 | fault in %: | 4.1007 | absolute : | 30.1543 |
| environment | 918.7600 | fault in %: | 3.7013 | absolute : | 34.0057 |